PERSPECTIVE
https://doi.org/10.1038/s44160-022-00115-3

nature synthesis

Design of soft matter for additive processing

Chun Lam Clement Chan[1], Jay Matthew Taylor[2] and Emily Catherine Davidson[1]✉

Digital assembly via extrusion-based additive manufacturing, or three-dimensional (3D) printing, grants the opportunity to attain exquisite control over material structure and composition at the local ('voxel') level. The synthetic incorporation of a diverse array of chemistries into 3D-printed soft materials has expanded its use into many application areas. However, substantial opportunity exists for synthesizing materials in which the functional microstructure (at both filler and molecular levels) interacts with the processing flows of extrusion-based manufacturing to achieve unique and enhanced properties. Here we articulate principles for designing and synthesizing soft materials with the potential to generate printed structures with superlative mechanical and stimuli-responsive properties. Specifically, we consider the rheological requirements of printing via direct ink writing and materials extrusion, and examine materials that show printing-directed alignment or trapping of tailored non-equilibrium structures. Finally, we discuss characterization approaches that connect filament-level microstructure with macroscopic behaviour, thus 'closing the loop' of material development. Collectively, these create the potential for additive manufacturing to achieve voxel-level control of composition, microstructure and properties.

Additive manufacturing techniques, which broadly enable the creation of structures by the 'addition' of material, have transformed multiple industries. They have allowed for the rapid prototyping and manufacturing of customized products, which encompass a broad variety of materials and applications. These range from customized orthodontics[1] to lightweight metallic parts for improved fuel efficiency in the aerospace industry[2] and three-dimensional (3D) visualizations of clinical imaging for diagnostics and surgery[3]. However, at present, most 3D printing (3DP) materials have been adapted from those used in traditional manufacturing techniques, constraining the flexibility and functionality that are currently achievable. Thus, great potential lies in synthesizing materials specifically for additive processing, which can be designed to interact synergistically with the unique processing conditions. We anticipate that leveraging this synergy to extend the capabilities of additive manufacturing to achieve voxel-level control—not just of composition, but also local material properties (such as orientation and microstructure)—will define the next generation of additive manufacturing.

To analyse and control the materials property of a manufactured part, it is necessary to understand not only the properties of the raw material (which in the case of soft materials is determined by chemistry), but also the assembly pathway (which is influenced by processing). Different processing techniques lead to varying shear, thermal, concentration, and compositional histories, which, in combination, direct the final materials properties. We envision that the future of additive manufacturing lies in materials custom-synthesized for additive processing to achieve the desired assembly pathway, such that the printing process itself can be considered an essential component of the material design. Achieving this goal will require an integrated understanding of how synthetic design impacts the evolution of material microstructure during printing, and how target form and microstructure maximize application-specific material properties (Fig. 1). Ultimately, this integrated understanding will allow for the iterative development of both materials and processing. In this Perspective we articulate design principles for digital assembly via extrusion-based additive processing, highlight materials that are designed and synthesized in accordance with these principles, and identify emergent opportunities.

Material design for extrusion-based 3D printing

To design materials for extrusion-based printing, it is important to understand how a material's structure responds to flow fields. Materials used in these printing processes span a number of material classes, from colloidal suspensions to polymer melts and gels. These systems possess microstructures of many forms, each of which is deformed and impacted differently by the shear and extensional flows intrinsic to printing processes (Fig. 2a,b). In some cases the change in microstructure enables extrusion of the materials and the original microstructure is rapidly recovered upon cessation of flow[4]. In others, changes in microstructure may persist following deposition, which can be leveraged as a desirable design tool[5,6]. Regardless, understanding how flow impacts the microstructure is critical to the intentional design and synthesis of printing materials. First, we discuss how molecular and microstructural design enables materials to (1) meet the basic rheological requirements for extrusion-based printing, (2) leverage printing flow fields for additional synergistic effects and (3) incorporate additional functionality to create responsive materials. Finally, we discuss approaches to explicitly probe the impact of printing on microstructures, linking microscale and macroscale properties and thereby enabling design feedback.

Rheological requirements of extrusion-based 3D printing. Materials must possess certain rheological characteristics to be printable via extrusion-based methods (broadly termed 'material extrusion'). Material extrusion encompasses approaches including both extrusion of viscoelastic 'inks', often termed 'direct ink writing' (DIW), as well as melt extrusion of pellet- or filament-based polymer feedstocks. Regardless of the approach, two requirements must be satisfied. First, materials must shear-thin to flow under applied stress, and then rapidly achieve solid-like properties upon exiting the nozzle[4,7]. Materials for DIW achieve these transitions via viscoelastic properties, often leveraging materials that exhibit a distinct yield stress (a stress-induced transition between solid-like and

[1]Department of Chemical and Biological Engineering, Princeton University, Princeton, NJ, USA. [2]Department of Materials Science and Engineering, University of Illinois Urbana-Champaign, Urbana, IL, USA. ✉e-mail: edavidson@princeton.edu

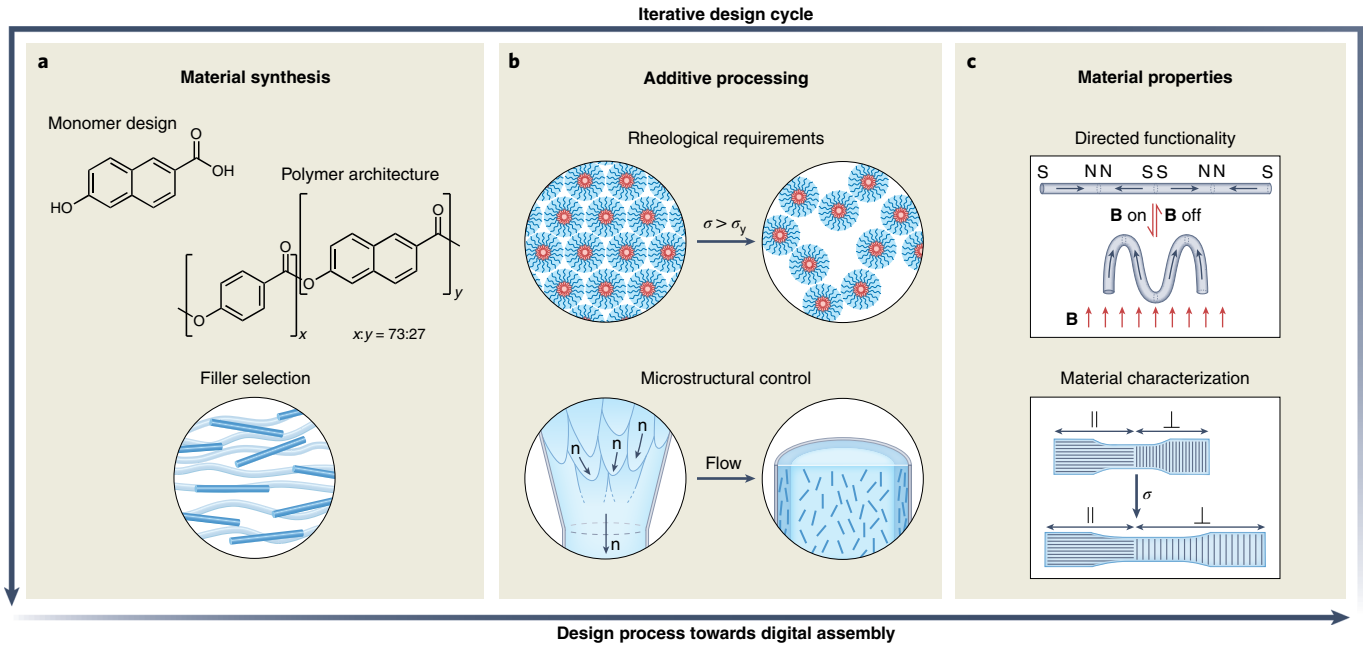

Fig. 1 | The design process to digital assembly by using extrusion-based additive processing. a, The first stage is material synthesis, encompassing monomer and polymer design as well as filler selection. **b**, During additive processing, the rheological requirements and the effects of flow on microstructure must be considered. For example, the rheological requirements for extrusion-based 3DP are met by the deformation of crystalline lattices of micelle-forming polymers upon application of stress exceeding the yield stress ($\sigma > \sigma_y$). In addition, microstructural control may be achieved, as exemplified by flow-driven alignment of liquid-crystalline (LC) polymers, which is represented by *n* (director, that is orientation, of the LC order)[41]. **c**, These stages culminate in the ability to target desired material properties and applications. These could include directed functionality, such as complex shape actuation upon application of a magnetic (**B**) field, and stress–strain behaviour that depends on the print path[53]. Future material design will require an integrated understanding of how synthetic design impacts the microstructure and material properties via processing pathways. Accordingly, detailed characterization linking the multiscale structure of a manufactured construct with its properties is essential. Figure adapted with permission from: **a**,**b**, ref. [41], Springer Nature Ltd; **c**, ref. [53], Springer Nature Ltd.

liquid-like properties). By contrast, melt extrusion from both filamentary and pellet polymer feedstocks relies on cooling-induced solidification[7,8]. Rapid solidification can also be achieved using photopolymerization[9]. Second, the material designer must consider the interfaces between filaments, as excellent adhesion is critical for final material properties. For example, thermoplastic polymer chains must diffuse sufficiently to achieve an entanglement density at interfaces that is comparable to that in the bulk[10,11], which is necessary to ensure sufficient weld strength and prevent gaps forming between printed filaments or 'roads'.

Shear-thinning and yield-stress behaviours can be designed by means of the material microstructure (Fig. 2b). Traditionally, DIW materials control these properties by incorporating particle networks, such as colloidal gels[12] (Fig. 2c) and percolating networks of fumed silica. Applying a stress above a critical value disrupts (yields) the gel's network structure, allowing flow. Following cessation of flow the network recovers, leading to solid-like properties. Furthermore, shear is concentrated at the walls of the extrusion nozzle[13–15], causing the material along the outside of the extrudate to yield while the core retains its solid-like properties. The retention of solid-like properties in the filament core during printing enables spanning and overhanging features[13]. Conversely, polymers used in melt extrusion achieve flow via heating followed by shear-induced chain alignment and loss of entanglements; rarely do these polymers exhibit classical yield stresses. However, these strategies are not always appropriate. Heating of entangled polymers offers few handles for control and can be inappropriate for materials that lack thermal stability. Similarly, introducing fillers is undesirable for many applications[16–18], and it can make the reuse and recycling of the printed part, critical to a circular plastics economy, challenging.

Instead of using fillers or applying heat, these critical rheological properties can be introduced by tailoring polymer–polymer interactions through rational chemical design and synthesis. For example, the incorporation of dynamic bonds, such as telechelic interactions[19], and supramolecular bonds[20,21], enables filler-free rheological control (Fig. 2d)[22], which has been exploited by the bioprinting community to synthesize printable hydrogels. Generally, the shear-sensitivity and, accordingly, the printability of the material are determined by the kinetics and density of reversible chemical associations. Notably, hydrogels of telechelic proteins demonstrate shear-thinning of three orders of magnitude, which, coupled with a rapid recovery, has enabled the production of self-supporting structures[19]. Studies employing supramolecular host–guest interactions have led to some of the most impressive work so far. For example, gels prepared from hyaluronic acid modified with either adamantane (guest) or β-cyclodextrin (host) side chains display shear-thinning and yielding at room temperature, followed by rapid recovery. High-fidelity printing of a host–guest modified hydrogel within another host–guest functionalized matrix hydrogel has also been demonstrated (Fig. 2d)[20]. This strategy allows for excellent shape fidelity, minimizes the shear forces experienced by embedded cells, and enables printing of embedded hydrogels. Yet, while these tailored associations can greatly improve printability, the mechanical properties of the printed structure are often insufficient for the final use and must be supplemented by additional processing steps, such as crosslinking (photo-[23] or thermally induced[24]) or initiating a phase transition (lower critical solution temperature, LCST)[25].

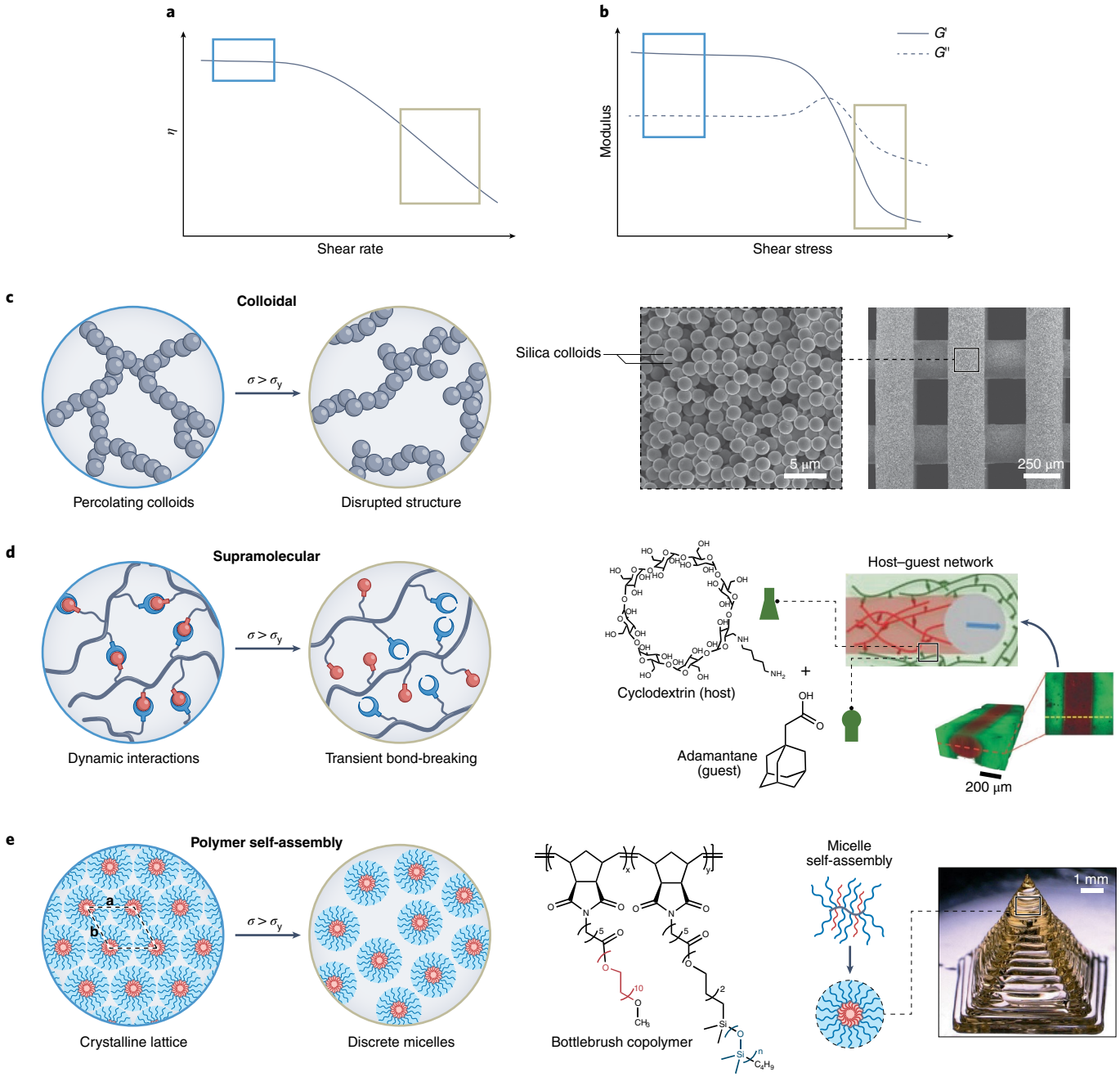

Fig. 2 | Designing yield stress interactions within the printing process. a,**b**, Representative plot of viscosity η (**a**) and storage and loss moduli (G′ and G′′, respectively) (**b**) as a function of shear stress. The blue and grey boxes represent shear conditions following and during extrusion, respectively. **c**, Left: schematic depicting the behaviour of a percolating colloidal network before and after application of stress exceeding the yield stress ($\sigma > \sigma_y$) to give a disrupted structure. Right: scanning electron microscopy (SEM) images of a colloidal silica network printed in a log-pile structure at two different magnifications[12]. **d**, Left: schematic showing dynamic chemical interactions before and after application of stress exceeding the yield stress ($\sigma > \sigma_y$). Right: for example, supramolecular interactions are formed between host (cyclodextrin) and guest (adamantane) when the ink (red) is extruded into a support gel (green). The resultant 3D structure is observed in fluorescence micrographs[20]. **e**, Left: schematic of crystalline lattices of micelle-forming polymers deforming upon application of stress exceeding the yield stress ($\sigma > \sigma_y$). Right: bottlebrush copolymers can self-assemble to form micelles that are subsequently printed to form supersoft structures composed of crosslinked bottlebrush copolymers. Figure adapted with permission from: **c**, ref. [12], Wiley; **d**, ref. [20], Wiley; **e**, ref. [18], under a Creative Commons licence CC BY 4.0.

Although to date the incorporation of dynamic bonds to tailor material rheology has been primarily utilized for the bioprinting of hydrogels, this approach offers substantial potential in the printing of both stimuli-responsive hydrogels and bulk polymers.

A variation of these strategies can be found in shear-sensitive micelle-forming block copolymers. The formed micelles can assemble into an ordered phase, where the elastic properties dominate in the quiescent state (Fig. 2e). Under shear, these interactions are interrupted, disrupting the positional order of the micelles (from a body-centred cubic crystal to disordered spheres) and enabling flow. Following cessation of shear, the structure and mechanical properties recover rapidly (Fig. 2e). These transitions have

been observed in amphiphilic block copolymers in aqueous solution (often referred to as pluronics), which have been extensively used as DIW inks[26–28]. At the appropriate concentration in water, pluronics assemble into micelles that exhibit the aforementioned shear-induced transformations[29]. In addition, pluronic hydrogels experience an LCST transition: upon cooling, the polymer chains become fully soluble in water and the gels liquify, enabling their evacuation as a sacrificial material[27]. Incorporation of additives or additional functional groups to pluronics has further enabled inks with optimized rheological properties, decreased polymer volume fraction, and capable of post-printing crosslinking to afford a robust final network[28]. Besides pluronics, shear-induced disordering transitions have similarly been observed for block-copolymer micelles in the bulk melt[18,30,31], which was exploited recently to achieve printable supersoft elastomers. A bulk polymer ink composed of short micelle-forming polydimethylsiloxane-polyethylene oxide bottlebrush copolymers was prepared. The ink could be printed at room temperature due to a shear-induced structural transition, fast relaxation dynamics and low glass transition temperature, and is also UV-crosslinkable, enabling post-printing transformation into a supersoft elastic solid (Fig. 2e)[18]. These characteristics would have been impossible if the required rheological behaviour was achieved using fillers as they would have interfered with the desired supersoft elasticity, and the bottlebrush molecular architecture was essential to achieve solid-like properties at room temperature[18].

Structures with dynamic, supramolecular, and/or telechelic interactions can not only satisfy the shear-thinning requirements of additive manufacturing, but also present significant potential for enhancing inter-filament adhesion. In particular, the self-healing properties characteristic of dynamic bonds can tune the material relaxation timescales and enable inter-filament bond formation. Ultimately, future opportunities exist to leverage polymer interactions to achieve bond association and dissociation at length scales (from molecular to mesoscale) and timescales relevant to additive processing.

Leveraging 3D printing for enhanced functionality. Beyond meeting the basic rheological requirements for printing, the forces acting on the materials during extrusion-based 3DP can also introduce additional functionality and tailor material properties. We are inspired by natural composites and biological materials whose superlative characteristics are not only a result of the heterogeneous properties of the constituent parts, but also the alignment of the underlying structure[32]. Extrusion-based additive manufacturing is uniquely poised to develop such hierarchically structured systems. First, although rapid recovery following flow-induced deformation is advantageous in achieving printability (by allowing fast solidification), a permanent change in microstructure can allow substantial synergy between printing and materials properties. The degree of material deformation can be understood by relating the stress field experienced by the material to the strength of the elastic response resisting deformation, which may be at the chain, domain interface or particle–particle interaction level. These microstructural changes in response to high shear-rate flows and high strain deformations can be monitored by rheological measurements, especially that of the normal stress differences[33,34]. Second, it is important to consider that microstructural deformation is sensitive to both the type, magnitude and duration of the applied stress field. Is the residence time of the material within the nozzle sufficient to induce the desired microstructural change?[15] Is the experienced flow fully shear in nature, or are there also substantial extensional components? Finally, upon removing the applied stress, permanent microstructural deformation may be achieved if the deformed structure is either more thermodynamically stable than the original one (with the printing process enabling the material to cross a kinetic barrier) or if the deformed structure is kinetically trapped by strategies such as crosslinking or rapid cooling.

A common method to take advantage of 'trapped' microstructures is to incorporate fillers, the orientations of which are preserved in a kinetically arrested state. The resulting tailored layout and orientation of aligned fillers, typically high-aspect-ratio nano- or micrometre-scale materials, have imparted enhanced mechanical properties and anisotropic stimuli response to printed materials (Fig. 3a,b). For example, silicon carbide aligned along the flow path in epoxy composites has enabled superlative Young's modulus values in printed cellular structures[35]. Cellulose, in the form of cellulose nanocrystals (CNCs) and cellulose nanofibrils (CNFs), has proven to be a particularly compelling filler for DIW owing to its sustainability and excellent mechanical and optical properties[36]. Printed structures composed of pure CNCs or CNC composites exhibit substantial programmable reinforcement via shear-induced alignment of CNCs along the print path[15,37,38]. Finally, manipulating the direction of processing flows relative to the print path is an exciting way to introduce local orientation (more specifically, orientation that is not only along the print path). A notable work describes the alignment of carbon fibres in epoxy using a rotating nozzle to achieve helical fibre orientation along the perimeter of each filament, resulting in printed samples with enhanced damage tolerance (Fig. 3a)[39]. With guidance from finite-element modelling tools, these approaches for materials design and printing offer a compelling opportunity for enhanced structural properties by leveraging processing flows.

These principles of printing-induced alignment can be extended to filler-free materials (Fig. 3b). In the simplest case, flow-induced chain anisotropy can be frozen by dropping below the glass transition, creating materials with tailored shape memory[40]. For example, in typical material extrusion methods, the nozzle shears along the surface of each filament or 'road' as it is deposited, leading to flattened cross-sections and a highly heterogeneous shear history. Parts can thus be designed to possess shape memory behaviour that exhibits bending as opposed to a uniform, contractile response. However, it should be noted that, if uncontrolled, the frozen-chain anisotropy can also lead to localized residual stress and warping of printed parts.

Extending beyond simple chain anisotropy, polymers exhibiting order at the chain–chain level, such as liquid-crystalline (LC) polymers, can further leverage the processing flows to introduce additional functionality (Fig. 3b). Although LC polymers possess anisotropic chain shapes, the chains lack long-range positional order and are characterized by their local orientation within domains. During printing, process flows exert forces on both the chains and domain interfaces, resulting in long-range alignment of the polymer (Fig. 3a,b, top schemes). In some cases, the local degree of alignment reflects the variation in process flows within the print nozzle. For example, the printing of Vectran, a thermotropic LC polymer, yields filaments with high molecular alignment at the outer shell layer and low alignment in the core[41]. This molecular alignment, in conjunction with the core–shell structure, leads to substantial mechanical anisotropy at the filament level (Fig. 3b, right images). When printed into more complex structures, Vectran exhibits improved toughness and inhibited crack propagation[41].

Recently, printing of optically active cholesteric LC polymers has demonstrated that locally controlled optical properties can similarly be achieved. The printed cholesteric phases are tilted at an angle dependent on the shear rate, leading to structures in which the local structural colour varies with viewing angle[42]. These principles of alignment for optical functionality may be further extended to solutions of nanostructured block copolymers: printing of polystyrene–polyisoprene–polystyrene block copolymers in toluene yields shear-aligned block-copolymer structures that, in turn, enhance alignment of optically active perovskite nanocrystals preferentially

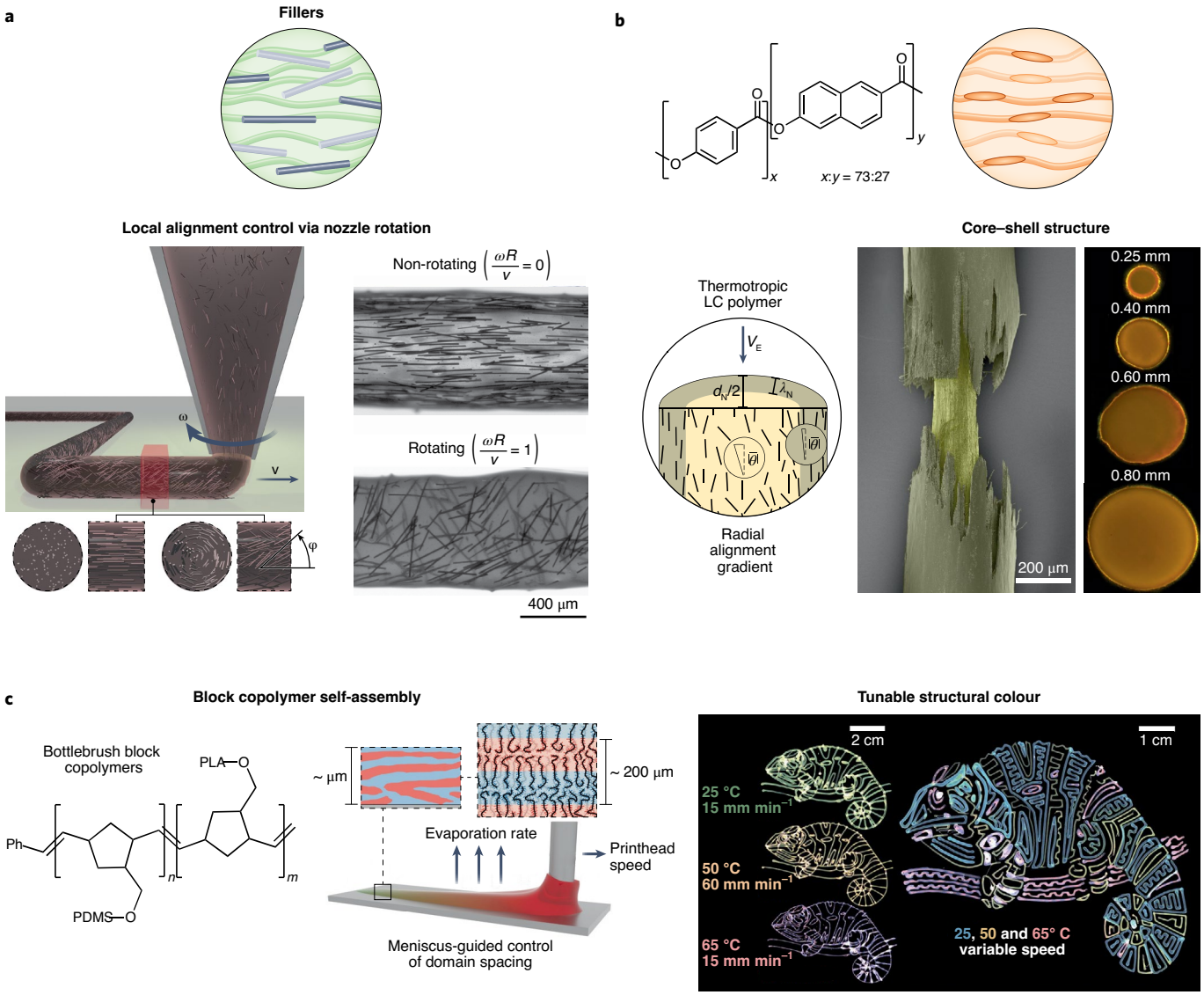

Fig. 3 | Imparting functionality during the printing process. a, Schematic (top) and an example of the alignment of fillers within 3D-printed networks (bottom). Epoxy resins with embedded carbon fibres are extruded out of a rotating nozzle. Fibre orientation is controlled by the rotation rate (ω), translational velocity (v) and nozzle radius (R), which impact the filament microstructure, as observed by comparing the filaments printed with and without rotation[39]. **b**, Schematic (top) and an example of the alignment of LC chemical groups within a 3D-printed polymer (bottom). LC polymer domains are aligned through printing (with extrusion speed V_E), leading to a core–shell structure of diameter d_N with a well-aligned shell (defined by thickness λ_N) and a disordered core. The alignment of the domains can be characterized by an average tilt $|\bar{\theta}|$. The nozzle size affects the structure of the printed filaments, as shown by the polarized optical microscopy images[41]. **c**, Schematic of meniscus-guided printing of bottlebrush polymers; the printhead speed and evaporation rate trap molecules in non-equilibrium domain spacings (left). On-the-fly control over domain spacing tailors the local colour of the printed pattern, as shown in the chameleon images (right)[6]. Figure adapted with permission from: **a**, ref. [39], National Academy of Sciences; **b**, ref. [41], Springer Nature Ltd; **c**, ref. [6], under a Creative Commons licence CC BY 4.0.

associated with polyisoprene domains[43]. There is great opportunity in developing inks containing such molecularly structured materials that, in concert with 3DP, exhibit controlled anisotropy of structure-associated optical, electrical and mechanical properties.

Additionally, precisely controlled printing processes can attain structures and functionalities beyond polymer or filler orientation. In many materials, application of specified shear can achieve targeted phase behaviour. For example, the application of certain shear flows dramatically reduces the timescales required for self-assembled lyotropic materials to transition into Frank–Kasper phases[44]. Besides accelerating the formation of equilibrium phases, the processing flows often allow access to highly non-equilibrium structures, which have been employed to great effect by leveraging meniscus-guided 3DP. For example, chiral semiconducting polymers that exhibit a helical backbone typically possess poor charge-transport properties under equilibrium self-assembly. Following high-shear processing via printing, the helical LC ordering can be suppressed, leading to planarized backbones and improved charge-transport properties[5]. Similarly, bottlebrush block copolymers that exhibit structural colour may be trapped into tailored domain spacings to achieve locally tuned structural colour (Fig. 3c)[6]. Thus, 3DP may trap materials in a metastable structure via non-equilibrium processing. Here, it is appropriate to consider 3DP as a tool for materials synthesis: by leveraging locally controlled processing

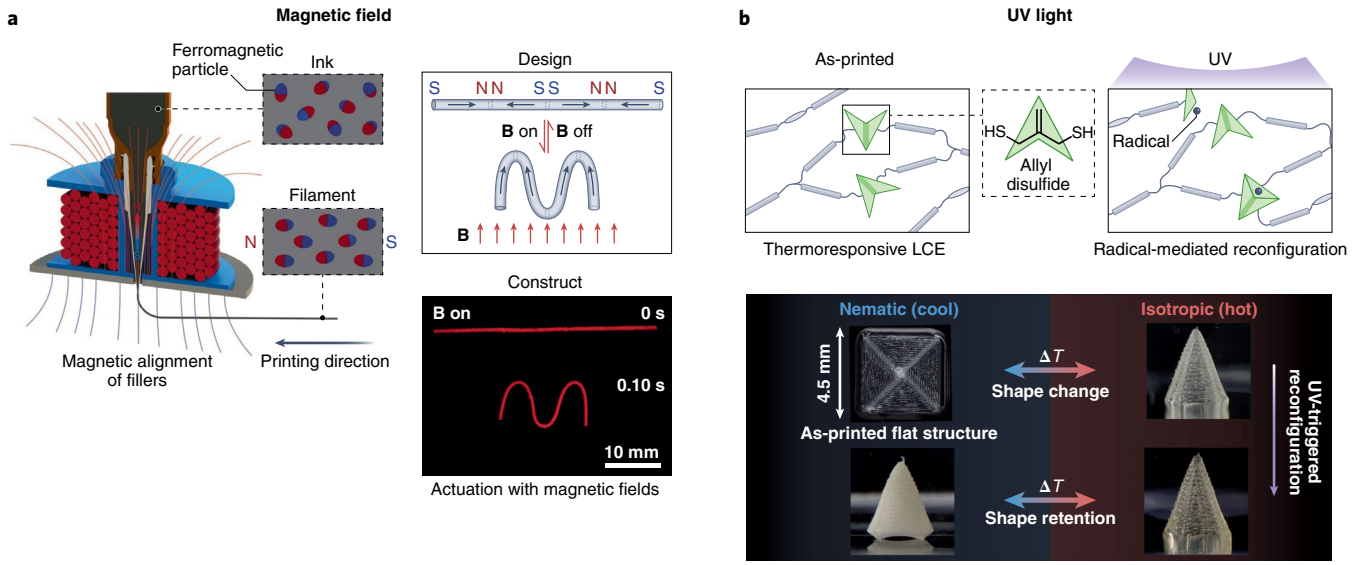

Fig. 4 | Controlling the functionality of 3D-printed material via external fields. a, Example of a filler-based responsive material, where magnetic particles are embedded in a silicone elastomer to control the local deformation of the structure in an applied magnetic field. The orientation of the magnetic fillers can be locally tailored during extrusion, which controls macroscopic deformation[53]. **b**, The preparation of a multi-stimuli-responsive material by incorporating two responsive chemistries into a single structure. A thermotropic LCE containing UV-initiated dynamic bonding segments (more specifically, allyl disulfide bonds) is used to first reversibly actuate the printed structure by heat, and then lock the deformed structure in place using UV light[57]. Figure adapted with permission from: **a**, ref. [53], Springer Nature Ltd; **b**, ref. [57], Wiley.

flows, 3DP can dictate microstructures and achieve properties inaccessible via other means.

Designing responsive materials for functional 3DP. 3D printing enables the integration of compositionally and structurally diverse responsive materials to achieve complex function. Substantial work has been devoted to develop materials that respond to a variety of stimuli, including light[45], mechanical force[46,47], electrical potential[48], humidity[38], pH[49], redox[50] and temperature[51], as well as more complex artificial molecular machines[52]. Translating stimuli-responsivity to printable materials requires referencing the aforementioned rheological design rules. Here we will focus on constructs in which functionality arises from the combination of stimuli-responsive materials synthesis, controlled fields during processing (for example, flow, magnetic or electric fields) and overall layout. Tailoring material functionality to respond to changes in the local environment yields benefits in the context of printed materials, from mechanoresponsive structures to actuators and soft robotics (Fig. 4).

Previously, we discussed the superlative mechanical properties achieved via flow-induced alignment of high-aspect-ratio fillers. This strategy can be extended to develop complex, stimuli-responsive architectures. For example, incorporating shear-aligned fillers into stimuli-responsive gels and elastomers can lead to shape-morphing structures of arbitrary complexity. Notably, alignment of CNFs in printed hydrogels enables an anisotropic swelling response along the print path, leading to on-demand shape change from flat printed structures to structures featuring complex regions of local curvature, such as a Calla lily[38]. Local orientation of fillers, that is, not solely along the print path, can be achieved by incorporating a responsive filler, allowing for additional control. An example of this approach is the printing of a silicone elastomer filled with ferromagnetic NdFeB microparticles that can be oriented by a strong, switchable magnetic field at the nozzle (Fig. 4a, top scheme). Spatial patterning of microparticle orientation in the printed structure leads to fast and reversible actuation in an applied magnetic field (Fig. 4a, bottom image)[53].

The potential of functional alignment extends to the molecular scale. Printing-driven alignment of LC polymers can achieve tunable stimuli-responsive properties (Fig. 4b). For example, alignment of LC polymer precursors followed by UV-crosslinking creates liquid-crystal elastomers (LCEs) with the molecular director oriented along the print path[54–56]. Thermoresponsive actuation leads to complex shape changes. Furthermore, synthetic design can be used to incorporate on-demand changes in behaviour and multi-stimuli response. For example, synthesis of an LCE with a second network of light-activated dynamic bonds allows reversible actuation until it is exposed to UV light in the actuated state (Fig. 4b). Light exposure 'locks in' the actuated state via stress–relaxation of the dynamic bonds[57]. The voxel-level control of multiple chemical moieties has enabled the creation of multifunctional, programmable materials using 3D printing. However, to attain a broader range of functionality, further research into materials synthesis, multi-responsive interactions and the role of processing flows on structure development is required.

Although multiple functions can be incorporated within a single material by synthetic design, extrusion-based 3DP also presents a powerful opportunity to leverage multimaterial layouts, both at the macroscopic (millimetre) length scale and by extending voxel control to a sub-filament level. In choosing and designing materials for such layouts, it is critical to consider the chemical design, dynamics and printing conditions required for excellent inter-material adhesion[8,58,59]. At the filament level, incorporating multiple materials, including stimuli-responsive elements, in core–shell architectures has enabled the creation of soft strain sensors[60], damage-tolerant lattices[61] and the precise control and integration of electrically responsive actuating elements[62,63]. Further flexibility can be achieved through heterogeneous layouts incorporating multiple filaments of different compositions, which display tremendous stimuli-responsivity via simple design principles. For example, when silicone elastomers are filled with glass fibres, their coefficient of thermal expansion differs greatly compared to those without any fillers. By coupling one filled and one unfilled filament in the form of curved bilayer ribs, printed lattices composed of these materials,

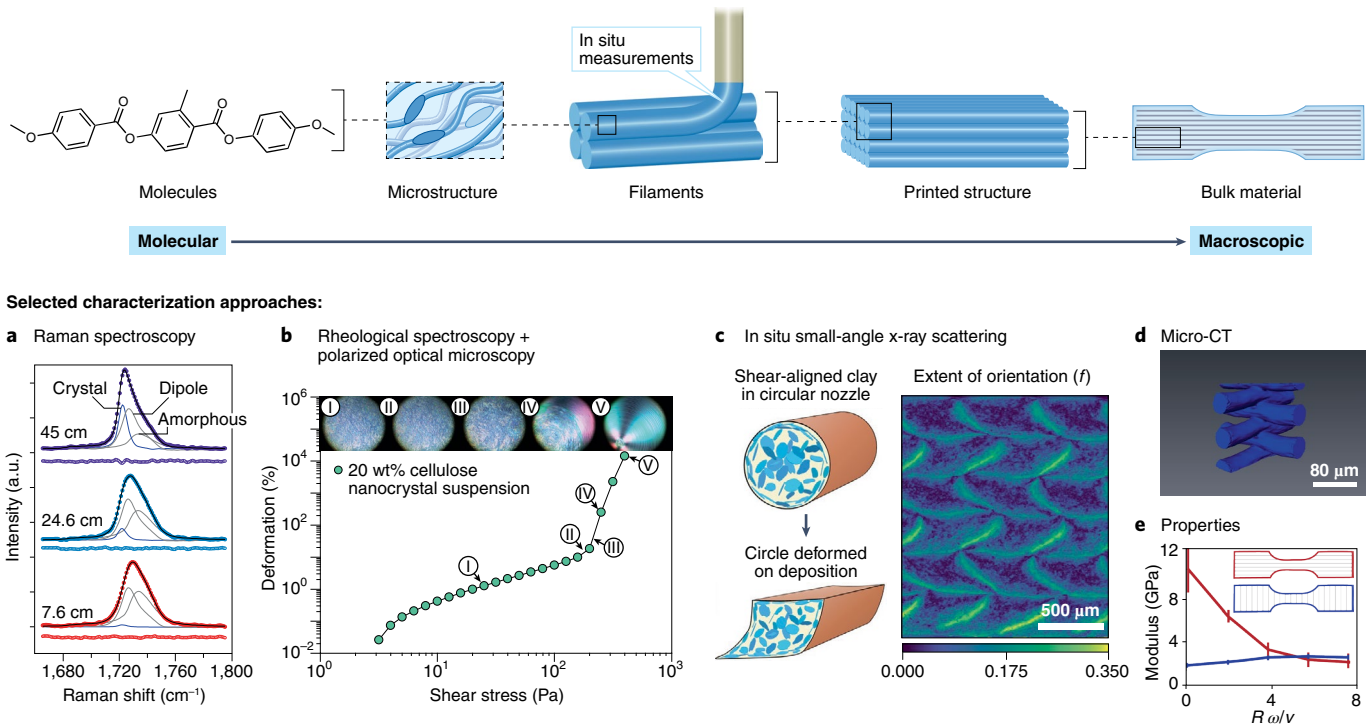

Fig. 5 | Characterization methods used in 3D printing for structural analysis at different length scales, from the molecular to the macroscopic scale. **a**, A representative plot of Raman spectroscopy showing an extruded polycaprolactone polymer measured at different distances from the nozzle. Each spectrum is deconvoluted to show the constituent spectra for crystalline, dipole–dipole and amorphous components of the curves[67]. **b**, A representative rheological plot showing the percentage deformation as a function of shear stress for a 20 wt% cellulose nanocrystal suspension, highlighting stages before (I), at (II) and after (III, IV) reaching the yield stress of the solution (corresponding polarized micrographs are shown at the top)[15]. **c**, Left: schematic of clay platelets aligned in a resin as a result of extrusion and its corresponding deformation after printing. Right: a plot of 3D microbeam X-ray scattering data showing the extent of orientation of the platelets within the printed structure[14]. Scale bar, 500 µm. **d**, X-ray micro-computed tomography image of a 3D-printed hydrogel-derived porous glass scaffold[73]. **e**, Differential modulus parallel (red line) and perpendicular (blue line) to the print path as a function of the non-dimensionalized rotation rate (defined in terms of nozzle radius R, rotational rate ω and translational velocity v) of a carbon-fibre reinforced epoxy ink printed using a rotating nozzle[39]. Figure adapted with permission from: **a**, ref. [67], Elsevier; **b**, ref. [15], American Chemical Society; **c**, ref. [14], Elsevier; **d**, ref. [73], Elsevier; **e**, ref. [39], National Academy of Sciences.

developed using inverse geometric design approaches, result in scalable temperature-responsive shape-shifting structures[64]. For more complex responses, printing that incorporates both stiff structural elements and multiple actuating LCEs with a range of phase-transition temperatures enables the creation of multi-stage origami structures, which can achieve multiple stable configurations in response to external stimuli. This approach has been used to manufacture a soft robot that assembles into a prism upon warming, and then rolls in the presence of a large temperature gradient between substrate and atmosphere[64]. Outstanding challenges in this area of multimaterial layouts lie in realizing excellent adhesion and tough, damage-resistant interfaces through a combination of layout architecture, processing, local composition and materials synthesis[65].

Connecting molecular and macroscopic structure

Printed materials exhibit substantial structural heterogeneity, both by design and as an unavoidable by-product of the gradients in flow profiles and (in some cases) the temperature intrinsic to extrusion-based 3DP. Characterizing this heterogeneity and understanding its contribution to the overall properties of the printed structure are critical steps towards closing the loop between design, processing and properties, allowing for an iterative design process towards targeted material applications. Techniques that can characterize local microstructure, orientation and heterogeneity at the filament level are of particular value for closing this loop (Fig. 5).

In this Perspective we have highlighted how extrusion-based printing can direct local microstructural anisotropy. A number of tools exist to probe this anisotropy. The degree of molecular anisotropy in printed polymers can be directly characterized using birefringence or polarized Raman measurements, which do not necessitate the high degree of order or crystallinity required by standard X-ray scattering measurements (Fig. 5a)[66,67]. In many cases, filler orientation can also be visualized using polarized optical imaging methods. For example, the orientation dynamics of CNCs have been measured via in situ parallel plate rheometry integrated with polarized light imaging. These measurements were used as a model to understand the evolution of shear-induced CNC particle alignment during 3DP by correlating the expected plug-flow radius with shear conditions (Fig. 5b)[15]. Polarized soft X-ray methods can similarly directly probe the molecular anisotropy, although they require specialized synchrotron facilities and ultra-thin samples due to the high absorption of the incident X-rays[68].

At larger length scales, microbeam X-ray scattering measurements (in which the beam cross-section is substantially smaller than the filament diameter) can also visualize the local microstructure and its heterogeneity, allowing us to develop models to rationalize material properties and the effects of the printing process. For example, recent work designed epoxy thermoset composites containing nanoclay and carbon-fibre fillers. Scanning microbeam X-ray scattering with extremely fine (5 µm) spatial resolution mapped the local orientational distribution of filler within both

individual printed filaments and collections of filaments, revealing substantial filler orientation at filament boundaries where high shear was experienced during extrusion and deposition (Fig. 5c)[14]. Microbeam studies have similarly been leveraged to characterize the orientational distribution and inter-mesogen distance of a smectic-A LC structure in 3D-printed LCEs[69], as well as the shear-induced formation of crystalline shish-kebab structures in the printing of isotactic polypropylene, probing differences in the development of crystalline microstructure within the printed filament core and at the interfaces[70]. Regardless of the method, techniques that measure orientation due to processing flows in two dimensions must take care in their conclusions concerning the full 3D distribution of orientations[71]. Additionally, we can anticipate future works in which flow-induced stress may cause, for example, microphase-separated polymers to be deformed from their equilibrium domain spacing. Depending on the distribution of flow within the extrusion nozzle, the balance of stresses experienced across the filament will vary, leading to a spatial heterogeneity in the degree of deviation from the equilibrium case. Again, advanced characterization tools such as microbeam X-ray scattering will play important roles in probing this multiscale heterogeneity. Macroscopic structure such as porosity size distribution (or lack thereof) can be captured by microscopy and confocal imaging, as well as more advanced techniques such as micro-computed tomography (Fig. 5d)[72,73]. Finally, specialized tools such as in situ X-ray photon correlation spectroscopy can directly probe changes in material dynamics during printing[74]; material designers can use this feedback to create materials with enhanced shape fidelity and inter-filament adhesion. Ultimately, the development of integrated tools that allow rapid characterization of microstructural heterogeneity in printed structures will be critical to enabling synthetic approaches to 'close the loop' and create targeted structure-level properties (Fig. 5e) by design.

Outlook

The field of additive manufacturing has seen remarkable growth in recent years and has shown opportunities not just for rapid prototyping, but in creating materials with properties and structures not accessible by other methods. In particular, through the control of materials properties at the voxel level, extrusion-based 3D printing has allowed the creation of oriented, heterogeneous materials with mechanical properties spanning many orders of magnitude, propelling forward its use in numerous applications.

In this Perspective we have highlighted key design approaches that we anticipate will be crucial themes for the future of the field. In particular, we have examined (1) key rheological properties for materials tailored to additive processing, (2) strategies for how printing can enhance and direct the microstructure for improved and tailored local properties relative to the bulk material and (3) approaches that leverage the interactions between materials and the printing process for stimuli-responsive and functional properties. Thus, it is important for chemical synthesis and additive processing to be considered in unison such that they interact synergistically. This strategy will yield materials with the necessary rheological behaviour for printing and the desired mechanical properties and/or chemical responsivity for the intended applications. Furthermore, the design process should be complemented by multiscale characterization methods to understand the effects of processing flows on the structure, heterogeneity and, ultimately, the macroscopic properties of the fabricated structure. Fully realizing these characterization approaches will require investment in shared user facilities with state-of-the art tools, which can simultaneously measure structure and dynamics across different length scales in printed materials. The development of such tools remains in its infancy. Accordingly, through synthesis, processing and characterization, we can achieve an iterative design cycle towards digital assembly via additive processing, where we can target specific materials composition and properties at the voxel level.

We expect that explicitly designing materials for additive processing will accelerate the pathway from material to product. Furthermore, as we advance our understanding of the relationship between materials design and properties, we can, in combination with theory, modelling, automation and in situ characterization of the relevant material and microstructural properties, reduce the trial and error required to achieve our desired goals and accelerate the design process. We expect that innovations in materials synthesis, in conjunction with the unique role of processing flows in enhancing and directing microstructure, will enable the next transformational advances in additive manufacturing.

Received: 25 February 2022; Accepted: 26 May 2022;
Published online: 5 August 2022

References

1. Wong, B. H. Invisalign A to Z. *Am. J. Orthod. Dentofacial Orthop.* **121**, 540–541 (2002).
2. Najmon, J. C., Raeisi, S. & Tovar, A. in *Additive Manufacturing for the Aerospace Industry* (eds Froes, F. & Boyer, R.) 7–31 (Elsevier, 2019).
3. Hosny, A. et al. From improved diagnostics to presurgical planning: high-resolution functionally graded multimaterial 3D printing of biomedical tomographic data sets. *3D Print. Addit. Manuf.* **5**, 103–113 (2018).
4. Nelson, A. Z. et al. Designing and transforming yield-stress fluids. *Curr. Opin. Solid State Mater. Sci.* **23**, 100758 (2019).
5. Park, K. S. et al. Tuning conformation, assembly and charge transport properties of conjugated polymers by printing flow. *Sci. Adv.* **5**, eaaw7757 (2019).
6. Patel, B. B. et al. Tunable structural color of bottlebrush block copolymers through direct-write 3D printing from solution. *Sci. Adv.* **6**, eaaz7202 (2020).
7. Truby, R. L. & Lewis, J. A. Printing soft matter in three dimensions. *Nature* **540**, 371–378 (2016).
8. Mackay, M. E. The importance of rheological behavior in the additive manufacturing technique material extrusion. *J. Rheol.* **62**, 1549–1561 (2018).
9. Zhu, J. Z., Zhang, Q., Yang, T. Q., Liu, Y. & Liu, R. 3D printing of multi-scalable structures via high penetration near-infrared photopolymerization. *Nat. Commun.* **11**, 3462 (2020).
10. McIlroy, C. & Olmsted, P. D. Disentanglement effects on welding behaviour of polymer melts during the fused-filament-fabrication method for additive manufacturing. *Polymer* **123**, 376–391 (2017).
11. Levenhagen, N. P. & Dadmun, M. D. Interlayer diffusion of surface segregating additives to improve the isotropy of fused deposition modeling products. *Polymer* **152**, 35–41 (2018).
12. Smay, J. E., Gratson, G. M., Shepherd, R. F., Cesarano, J. & Lewis, J. A. Directed colloidal assembly of 3D periodic structures. *Adv. Mater.* **14**, 1279–1283 (2002).
13. Smay, J. E., Cesarano, J. & Lewis, J. A. Colloidal inks for directed assembly of 3-D periodic structures. *Langmuir* **18**, 5429–5437 (2002).
14. Trigg, E. B. et al. Revealing filler morphology in 3D-printed thermoset nanocomposites by scanning microbeam X-ray scattering. *Addit. Manuf.* **37**, 101729 (2021).
15. Hausmann, M. K. et al. Dynamics of cellulose nanocrystal alignment during 3D printing. *ACS Nano* **12**, 6926–6937 (2018).
16. Wang, C., Rubakhin, S. S., Enright, M. J., Sweedler, J. V. & Nuzzo, R. G. 3D particle-free printing of biocompatible conductive hydrogel platforms for neuron growth and electrophysiological recording. *Adv. Funct. Mater.* **31**, 2010246 (2021).
17. Rauzan, B. M., Nelson, A. Z., Lehman, S. E., Ewoldt, R. H. & Nuzzo, R. G. Particle-free emulsions for 3D printing elastomers. *Adv. Funct. Mater.* **28**, 1707032 (2018).
18. Xie, R. et al. Room temperature 3D printing of super-soft and solvent-free elastomers. *Sci. Adv.* **6**, eabc6900 (2020).
19. Olsen, B. D., Kornfield, J. A. & Tirrell, D. A. Yielding behavior in injectable hydrogels from telechelic proteins. *Macromolecules* **43**, 9094–9099 (2010).
20. Highley, C. B., Rodell, C. B. & Burdick, J. A. Direct 3D printing of shear-thinning hydrogels into self-healing hydrogels. *Adv. Mater.* **27**, 5075–5079 (2015).
21. Sather, N. A. et al. 3D printing of supramolecular polymer hydrogels with hierarchical structure. *Small* **17**, 2005743 (2021).
22. Lee, S. C., Gillispie, G., Prim, P. & Lee, S. J. Physical and chemical factors influencing the printability of hydrogel-based extrusion bioinks. *Chem. Rev.* **120**, 10797–10849 (2020).
23. Ouyang, L., Highley, C. B., Rodell, C. B., Sun, W. & Burdick, J. A. 3D printing of shear-thinning hyaluronic acid hydrogels with secondary cross-linking. *ACS Biomater. Sci. Eng.* **2**, 1743–1751 (2016).

24. Nadgorny, M., Collins, J., Xiao, Z., Scales, P. J. & Connal, L. A. 3D-printing of dynamic self-healing cryogels with tuneable properties. *Polym. Chem.* **9**, 1684–1692 (2018).
25. Cai, L., Dewi, R. E. & Heilshorn, S. C. Injectable hydrogels with in situ double network formation enhance retention of transplanted stem cells. *Adv. Funct. Mater.* **25**, 1344–1351 (2015).
26. Zhang, M. et al. Hierarchical-coassembly-enabled 3D-printing of homogeneous and heterogeneous covalent organic frameworks. *J. Am. Chem. Soc.* **141**, 5154–5158 (2019).
27. Kolesky, D. B. et al. 3D bioprinting of vascularized, heterogeneous cell-laden tissue constructs. *Adv. Mater.* **26**, 3124–3130 (2014).
28. Zhang, M. S. et al. Dual-responsive hydrogels for direct-write 3D printing. *Macromolecules* **48**, 6482–6488 (2015).
29. Newby, G. E., Hamley, I. W., King, S. M., Martin, C. M. & Terrill, N. J. Structure, rheology and shear alignment of pluronic block copolymer mixtures. *J. Colloid Interface Sci.* **329**, 54–61 (2009).
30. Sebastian, J. M., Lai, C., Graessley, W. W. & Register, R. A. Steady-shear rheology of block copolymer melts and concentrated solutions: disordering stress in body-centered-cubic systems. *Macromolecules* **35**, 2707–2713 (2002).
31. Xie, R. et al. Yielding behavior of bottlebrush and linear block copolymers. *Macromolecules* **54**, 5636–5647 (2021).
32. Fratzl, P. & Weinkamer, R. Nature's hierarchical materials. *Prog. Mater. Sci.* **52**, 1263–1334 (2007).
33. Wagner, N. J. & Mewis, J. in *Theory and Applications of Colloidal Suspension Rheology Cambridge Series in Chemical Engineering* (eds Mewis, J. & Wagner, N. J.) 1–43 (Cambridge Univ. Press, 2021).
34. Baek, S. G., Magda, J. J. & Larson, R. G. Rheological differences among liquid-crystalline polymers. I. The first and second normal stress differences of PBG solutions. *J. Rheol.* **37**, 1201–1224 (1993).
35. Compton, B. G. & Lewis, J. A. 3D-printing of lightweight cellular composites. *Adv. Mater.* **26**, 5930–5935 (2014).
36. Frka-Petesic, B. & Vignolini, S. So much more than paper. *Nat. Photon.* **13**, 365–367 (2019).
37. Siqueira, G. et al. Cellulose nanocrystal inks for 3D printing of textured cellular architectures. *Adv. Funct. Mater.* **27**, 1604619 (2017).
38. Sydney Gladman, A., Matsumoto, E. A., Nuzzo, R. G., Mahadevan, L. & Lewis, J. A. Biomimetic 4D printing. *Nat. Mater.* **15**, 413–418 (2016).
39. Raney, J. R. et al. Rotational 3D printing of damage-tolerant composites with programmable mechanics. *Proc. Natl Acad. Sci. USA* **115**, 1198–1203 (2018).
40. Zhang, Q., Yan, D., Zhang, K. & Hu, G. Pattern transformation of heat-shrinkable polymer by three-dimensional (3D) printing technique. *Sci. Rep.* **5**, 8936 (2015).
41. Gantenbein, S. et al. Three-dimensional printing of hierarchical liquid–crystal–polymer structures. *Nature* **561**, 226–230 (2018).
42. Sol, J. A. H. P. et al. Anisotropic iridescence and polarization patterns in a direct ink written chiral photonic polymer. *Adv. Mater.* **33**, 2103309 (2021).
43. Zhou, N. et al. Perovskite nanowire-block copolymer composites with digitally programmable polarization anisotropy. *Sci. Adv.* **5**, eaav8141 (2019).
44. Valentine, C. S., Jayaraman, A., Mahanthappa, M. K. & Walker, L. M. Shear-modulated rates of phase transitions in sphere-forming diblock oligomer lyotropic liquid crystals. *ACS Macro Lett.* **10**, 538–544 (2021).
45. Jiang, H. Y., Kelch, S. & Lendlein, A. Polymers move in response to light. *Adv. Mater.* **18**, 1471–1475 (2006).
46. Li, J., Nagamani, C. & Moore, J. S. Polymer mechanochemistry: from destructive to productive. *Acc. Chem. Res.* **48**, 2181–2190 (2015).
47. Epstein, E., Kim, T. A., Kollarigowda, R. H., Sottos, N. R. & Braun, P. V. Force-modulated equilibria of mechanophore-metal coordinate bonds. *Chem. Mater.* **32**, 3869–3878 (2020).
48. Park, T. J. et al. Electrically tunable soft-solid block copolymer structural color. *ACS Nano* **9**, 12158–12167 (2015).
49. Kocak, G., Tuncer, C. & Bütün, V. pH-responsive polymers. *Polym. Chem.* **8**, 144–176 (2017).
50. Kramer, J. R. & Deming, T. J. Glycopolypeptides with a redox-triggered helix-to-coil transition. *J. Am. Chem. Soc.* **134**, 4112–4115 (2012).
51. Liu, R., Fraylich, M. & Saunders, B. R. Thermoresponsive copolymers: from fundamental studies to applications. *Colloid. Polym. Sci.* **287**, 627–643 (2009).
52. Lancia, F., Ryabchun, A. & Katsonis, N. Life-like motion driven by artificial molecular machines. *Nat. Rev. Chem.* **3**, 536–551 (2019).
53. Kim, Y., Yuk, H., Zhao, R., Chester, S. A. & Zhao, X. Printing ferromagnetic domains for untethered fast-transforming soft materials. *Nature* **558**, 274–279 (2018).
54. Kotikian, A., Truby, R. L., Boley, J. W., White, T. J. & Lewis, J. A. 3D printing of liquid crystal elastomeric actuators with spatially programed nematic order. *Adv. Mater.* **30**, 1706164 (2018).
55. Ambulo, C. P. et al. Four-dimensional printing of liquid crystal elastomers. *ACS Appl. Mater. Interfaces* **9**, 37332–37339 (2017).
56. López-Valdeolivas, M., Liu, D., Broer, D. J. & Sánchez-Somolinos, C. 4D printed actuators with soft-robotic functions. *Macromol. Rapid Commun.* **39**, 1700710 (2018).
57. Davidson, E. C., Kotikian, A., Li, S., Aizenberg, J. & Lewis, J. A. 3D printable and reconfigurable liquid crystal elastomers with light-induced shape memory via dynamic bond exchange. *Adv. Mater.* **32**, 1905682 (2020).
58. Coasey, K., Hart, K. R., Wetzel, E., Edwards, D. & Mackay, M. E. Nonisothermal welding in fused filament fabrication. *Addit. Manuf.* **33**, 101140 (2020).
59. Hart, K. R. et al. Increased fracture toughness of additively manufactured amorphous thermoplastics via thermal annealing. *Polymer* **144**, 192–204 (2018).
60. Frutiger, A. et al. Capacitive soft strain sensors via multicore-shell fiber printing. *Adv. Mater.* **27**, 2440–2446 (2015).
61. Mueller, J., Raney, J. R., Shea, K. & Lewis, J. A. Architected lattices with high stiffness and toughness via multicore-shell 3D printing. *Adv. Mater.* **30**, 1705001 (2018).
62. Kotikian, A. et al. Innervated, self-sensing liquid crystal elastomer actuators with closed loop control. *Adv. Mater.* **33**, 2101814 (2021).
63. Chortos, A. et al. Printing reconfigurable bundles of dielectric elastomer fibers. *Adv. Funct. Mater.* **31**, 2010643 (2021).
64. Boley, J. W. et al. Shape-shifting structured lattices via multimaterial 4D printing. *Proc. Natl Acad. Sci. USA* **116**, 20856–20862 (2019).
65. Wang, Z. et al. Stretchable materials of high toughness and low hysteresis. *Proc. Natl Acad. Sci. USA* **116**, 5967–5972 (2019).
66. Hassan, N. M., Migler, K. B., Hight Walker, A. R., Kotula, A. P. & Seppala, J. E. Comparing polarized Raman spectroscopy and birefringence as probes of molecular scale alignment in 3D printed thermoplastics. *MRS Commun.* **11**, 157–167 (2021).
67. Northcutt, L. A., Orski, S. V., Migler, K. B. & Kotula, A. P. Effect of processing conditions on crystallization kinetics during materials extrusion additive manufacturing. *Polymer* **154**, 182–187 (2018).
68. Collins, B. A. et al. Polarized X-ray scattering reveals non-crystalline orientational ordering in organic films. *Nat. Mater.* **11**, 536–543 (2012).
69. Prévôt, M. E. et al. Synchrotron microbeam diffraction studies on the alignment within 3D-printed smectic-A liquid crystal elastomer filaments during extrusion. *Crystals* **11**, 523 (2021).
70. Shmueli, Y. et al. In situ time-resolved X-ray scattering study of isotactic polypropylene in additive manufacturing. *ACS Appl. Mater. Interfaces* **11**, 37112–37120 (2019).
71. Corona, P. T. et al. Bayesian estimations of orientation distribution functions from small-angle scattering enable direct prediction of mechanical stress in anisotropic materials. *Phys. Rev. Mater.* **5**, 065601 (2021).
72. Visser, C. W., Amato, D. N., Mueller, J. & Lewis, J. A. Architected polymer foams via direct bubble writing. *Adv. Mater.* **31**, 1904668 (2019).
73. Fu, Q., Saiz, E. & Tomsia, A. P. Direct ink writing of highly porous and strong glass scaffolds for load-bearing bone defects repair and regeneration. *Acta Biomater.* **7**, 3547–3554 (2011).
74. Yavitt, B. M. et al. Revealing nanoscale dynamics during an epoxy curing reaction with X-ray photon correlation spectroscopy. *J. Appl. Phys.* **127**, 114701 (2020).

Acknowledgements

We thank J. A. Lewis for helpful discussions. This work was partially supported by the MRSEC programme of the National Science Foundation (DMR-2011750) through the Princeton Center for Complex Materials. J.M.T. acknowledges support from an ARO MURI award (no. W911NF-17-1-0351).

Author contributions

This perspective was conceived by E.C.D., and written by C.L.C.C., E.C.D. and J.M.T.

Competing interests

The authors declare no competing interests.

Additional information

Correspondence should be addressed to Emily Catherine Davidson.

Peer review information *Nature Synthesis* thanks the anonymous reviewers for their contribution to the peer review of this work. Primary Handling Editor: Alison Stoddart, in collaboration with the *Nature Synthesis* team.